



Topological insulator behavior of WS₂ monolayer with square-octagon ring structure

Ashok Kumar, Ravindra Pandey, P. K. Ahluwalia, and K. Tankeshwar

Citation: [AIP Conference Proceedings](#) **1731**, 140049 (2016); doi: 10.1063/1.4948215

View online: <http://dx.doi.org/10.1063/1.4948215>

View Table of Contents: <http://scitation.aip.org/content/aip/proceeding/aipcp/1731?ver=pdfcov>

Published by the [AIP Publishing](#)

Articles you may be interested in

[Plasmon-phonon coupling in monolayer WS₂](#)

Appl. Phys. Lett. **108**, 131903 (2016); 10.1063/1.4944948

[Tunneling transport in a few monolayer-thick WS₂/graphene heterojunction](#)

Appl. Phys. Lett. **105**, 223109 (2014); 10.1063/1.4903190

[First-principles study of graphene adsorbed on WS₂ monolayer](#)

J. Appl. Phys. **114**, 183709 (2013); 10.1063/1.4829483

[Mechanically strained tuning of the electronic and dielectric properties of monolayer honeycomb structure of tungsten disulphide\(WS₂\)](#)

AIP Conf. Proc. **1512**, 1242 (2013); 10.1063/1.4791501

[Electronic and optical properties of vacancy-doped WS₂ monolayers](#)

AIP Advances **2**, 042141 (2012); 10.1063/1.4768261

Topological Insulator Behavior of WS₂ Monolayer with Square-octagon Ring Structure

Ashok Kumar^{1*}, Ravindra Pandey², P. K. Ahluwalia³ and K. Tankeshwar⁴

¹ Centre for Physical Sciences, School of Basic and Applied Sciences, Central University of Punjab, Bathinda, India 151001

²Department of Physics, Michigan Technological University Houghton, MI, USA

³Department of Physics, Himachal Pradesh University Shimla, India, 171005

⁴Department of Physics, Panjab University Chandigarh, India 160014

*email: ashok@cup.ac.in

Abstract. We report electronic behavior of an allotrope of monolayer WS₂ with a square octagon ring structure, referred to as (so-WS₂) within state-of-the-art density functional theory (DFT) calculations. The WS₂ monolayer shows semi-metallic characteristics with Dirac-cone like features around Γ . Unlike p-orbital's Dirac-cone in graphene, the Dirac-cone in the so-WS₂ monolayer originates from the d-electrons of the W atom in the lattice. Most interestingly, the spin-orbit interaction associated with d-electrons induce a finite band-gap that results into the metal-semiconductor transition and topological insulator-like behavior in the so-WS₂ monolayer. These characteristics suggest the so-WS₂ monolayer to be a promising candidate for the next-generation electronic and spintronics devices.

Keywords: Monolayer, TMDs, Electronic Structure, DFT, Topological Insulator

PACS: 71.15.-m, 71.20.-b, 73.22.-f, 64.60.-i

INTRODUCTION

Transition metal dichalcogenides (TMDs) monolayers such as MoS₂[1-2] have emerged as most interesting two dimensional (2D) materials due to their unique mechanical, electronic and optical properties that show tunability with external electric field and mechanical strain [3-6]. 2D TMDs generally possess exotic properties in hexagonal (H) and trigonal (T) phase [7-8], however, it has been recently shown that monolayer TMDs can become 2D topological insulators (TIs) when they transform into 1T' structure [9].

Recently, energetically and thermodynamically stable allotrope of monolayer MoS₂ namely *so-MoS₂* has been found to possess graphene-like Dirac cone structure that opens up the possibilities for developing high performance electronic and spintronic devices [10]. Distinct from graphene, monolayer *so-MoS₂* possess d-electron Dirac fermions which has Fermi velocity comparable with graphene.

Inspired by the above study, in this paper, we present electronic behavior of *so-WS₂* monolayer with

and without spin-orbit coupling (SOC) effect, within the state-of-art density functional theory (DFT) based calculations.

COMPUTATIONAL DETAILS

DFT calculations are performed using Projector-Augmented Wave (PAW) pseudopotential implementation of Vienna Ab-initio Simulation Package (VASP)[11]. The electrons exchange and correlation effects are described by generalized gradient approximation (GGA) functional of Perdew-Burke-Ernzerhof (PBE). Kohn-Sham wave functions are expanded in a plane-wave basis set with a kinetic energy cutoff of 400 eV on a (20 × 20 × 1) Monkhorst-Pack grid using Gaussian smearing of 100 meV. A 25 Å vacuum region perpendicular to monolayer is used to overcome the interaction between periodic images.

RESULTS AND DISCUSSIONS

The *so-WS₂* monolayer consists of repeated square-octagon (so) rings in a square lattice as shown in

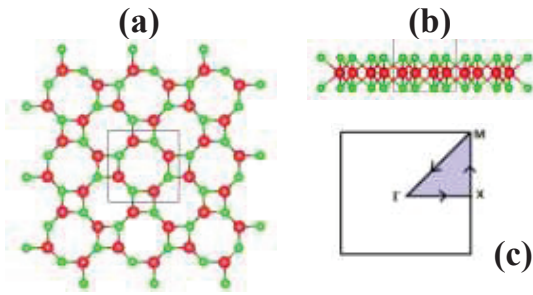


FIGURE 1. Crystal structure of the so-WS₂ monolayer : (a) top view (b) side view. Red circles represent W atoms and green circles represent S atoms. Unit cell is shown by solid lines. (c) The Brillouin zone with high symmetry paths.

Figure 1 (a and b). The primitive cell of so-WS₂ contains four W and eight S atoms in square bravais lattice with $p4$ symmetry. Note that most stable phase of WS₂ is hexagonal (H) with $p6m$ symmetry that contain one W and two S atoms per primitive cell [3].

Similar to the monolayer H-WS₂ which form six-member ring i.e. hexagons, so-WS₂ can be seen as triatomic layer where W atom is sandwiched between the two S planes to form eight-member ring (Figure 1). Note that eight-member and four-member ring in TMDs are found to posses at the grain boundaries of H-MX₂ monolayers [12].

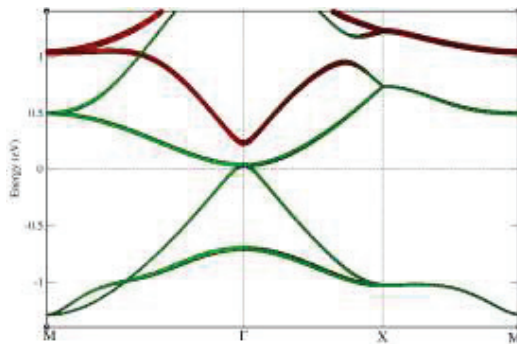


FIGURE 2.Orbitals-resolved electronic band structure of the so-WS₂ monolayer. Red color represents contributions from $d_{x^2-y^2}/d_{xy}$ orbitals and green color represents contributions from d_{z^2} orbitals of W atom. Fermi level is set at 0 eV.

Our calculated lattice constant of the so-WS₂ monolayer is 6.37 Å which is nearly same (6.36 Å) as reported for so-MoS₂ [10]. Despite nearly equal lattice constant, their electronic band structure show distinctly different features in terms of bands dispersion. Note that electronic band structure was calculated along M-Γ-X-M high symmetry directions of a square Brillouin zone [Figure 1(c)]. Valance band maximum (VBM), conduction band minimum (CBM) and CBM+1 are well separated from VBM and CBM

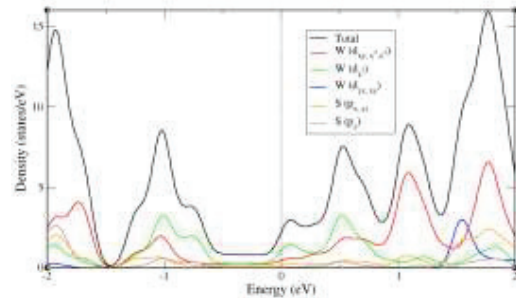


FIGURE 3. Total and partial density of states of the so-WS₂ monolayer. Fermi level is set at 0 eV.

(Figure 2) at Γ, whereas these points meet at a single Dirac point in so-MoS₂ monolayer [10]. However, in both the band structures, semi-metallic characteristics with Dirac-cone like features in VBM and CBM+1 at Γ (Figure 2) is observed.

In the so-WS₂ monolayer, $d_{x^2-y^2}/d_{xy}$ and d_{yz}/d_{xz} orbitals of W are doubly degenerated in energy while d_{z^2} is singly degenerated. VBM is mainly composed of d_{z^2} orbitals of W with small contributions from $d_{x^2-y^2}/d_{xy}$ orbitals, CBM is mainly contributed from d_{z^2} orbitals of W atoms. Similarly, CBM+1 at Γ has primary contributions from $d_{x^2-y^2}/d_{xy}$ orbitals of W atoms. It is found that S atoms and d_{yz}/d_{xz} orbitals of

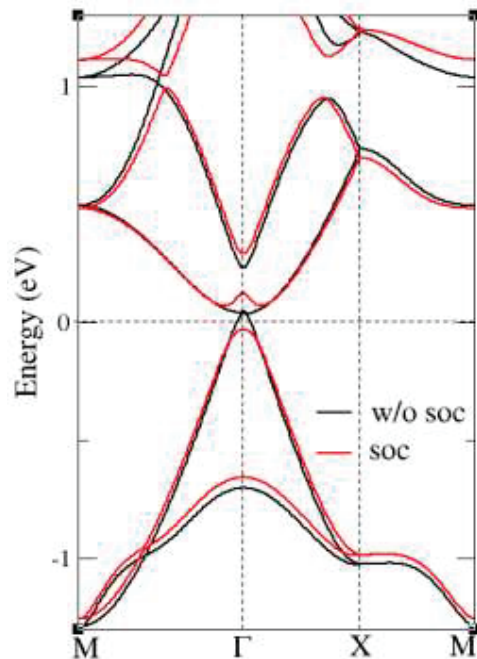


FIGURE 4. Electronic band structure of the so-WS₂ monolayer with and without the spin-orbit coupling (soc) effect.

W have negligible contributions at VBM, CBM and CBM+1 levels. These observations are in line with the so-MoS₂ monolayer [10]. The metallic character of so-WS₂ is also supported by the metallic density of states near Fermi energy (Figure 3). Significant hybridization of S states with d states of W has been found above 1 eV from Fermi level in both valence and conduction bands.

Most interestingly, by turning on the spin-orbit coupling (SOC) effect, VBM and CBM at Γ shifts downward and upward respectively inducing band-gap that results into the metal-semiconductor transition (Figure 4). The SOC-induced band-gap opening strongly suggests the so-WS₂ monolayer to be a two-dimensional topological insulator. The band-gap originates from the strong spin-orbit interactions of the d-electrons of W atoms around the Fermi energy.

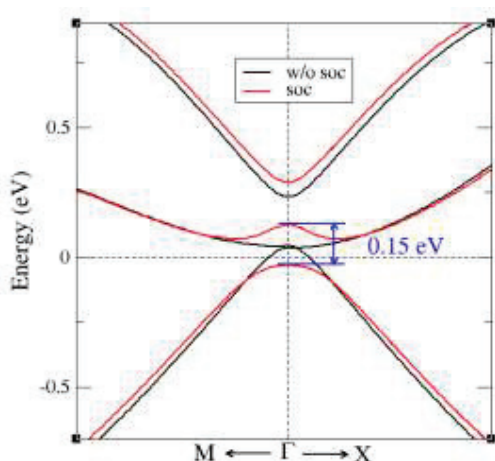


FIGURE 5. Electronic band dispersion and SOC induced band gap in the vicinity of Γ .

The SOC-induced splitting between degenerate bands at Γ results into 150 meV band-gap in the so-WS₂ monolayer (Figure 5). It is found that the SOC effect splits VBM and CBM as large as 65 and 85 meV, respectively at Γ . Similarly, CBM+1 and VBM-1 levels get shifted by 50 and 40 meV, respectively. Conical features at VBM and CBM+1 levels at Γ get flattened (as shown in Figure 5) when we turn on the SOC effects, indicating the existence of heavy fermions at Γ along with massless Dirac fermions in the direction of Γ -X and Γ -M due to linear band dispersions in the Brillouin zone.

CONCLUSIONS

In conclusions, first principles calculations have been performed to investigate the electronic behavior

of monolayer WS₂ with the square-octagon ring bravais lattice. The so-WS₂ monolayer is found to be semi-metallc with Dirac-cone like features around Γ . The SOC effects induced \sim 150 meV band-gap, thereby, suggesting so-WS₂ to be 2D topological insulator. Our study suggests that engineering the lattice of WS₂ and other 2D TMDs may found promising applications in the area of spintronics, photonics and high performance electronics.

ACKNOWLEDGMENTS

Superior, a high performance computing cluster at Michigan Technological University, was used in obtaining results presented in this paper.

REFERENCES

1. A. Kumar and P. K. Ahluwalia " Tunable Electronic and Dielectric Properties of Molybdenum Disulfide" in *MoS₂: Materials, Physics, and Device*, edited by Z. M. Wang, Switzerland : Springer International Publishing, 2014, pp. 53-76.
2. A. Kumar and P. K. Ahluwalia, *Mater. Chem. Phys.* **135**, 755-761 (2012).
3. A. Kumar and P. K. Ahluwalia, *Euro Phys J B* **85**, 186 (2012).
4. A. Kumar and P. K. Ahluwalia, *Physica B* **407**, 4627-4634 (2012); *ibid* **419**, 66-75 (2013).
5. A. Kumar and P. K. Ahluwalia, *Model. Simul. Mater. Sci. Enginer.* **21**, 065015 (2013).
6. A. Kumar and P. K. Ahluwalia, *J. Alloys Comps.* **550**, 283-291 (2013); *ibid* **587**, 459-467 (2014).
7. K. N. Duerloo, Y. Li and E. J. Reed, *Nat. Commun.* **5**, 4214 (2014).
8. A. Kumar, H. He, R. Pandey, P. K. Ahluwalia and K. Tankeshwar, *Phys.Chem. Chem. Phys.* **17**, 19215-19221 (2015).
9. X. Qian, J. Liu, L. Fu and J. Li, *Science* **346**, 1344-1347 (2014).
10. W. Li, M. Guo, G. Zhang and Y. Zhang, *Phys. Rev. B* **89**, 205402 (2014).
11. G. Kresse and J. Furthmuller, *Phys. Rev. B.* **54**, 11169-11186 (1996).
12. A. M. Zande, P. Y. Huang, D. A. Chenet, T. C. Berkelbach, Y. You, G. Lee, T. F. Heinz, D. R. Reichman, D. A. Muller and J. C. Hone, *Nat. Mater.* **12**, 554 (2013).